

RF COMMISSIONING AND PERFORMANCE IN THE CBETA ERL*

N. Banerjee[†], K. Deitrick, J. Dobbins, G. Hoffstaetter, R. Kaplan, M. Liepe,
 C. Miller, P. Quigley, E. Smith, V. Veshcherevich,
 Cornell Laboratory for Accelerator-Based Sciences and Education, Ithaca, USA

Abstract

The Cornell-BNL ERL Test Accelerator (CBETA) is a new multi-turn energy recovery linac currently being commissioned at Cornell University. It uses a superconducting main linac to accelerate electrons by 36 MeV and recover their energy. The energy recovery process is sensitive to fluctuations in the accelerating field of all cavities. In this paper, we outline our semi-automated RF commissioning procedure, which starts from automatic coarse tuning of the cavity all the way to adjusting the field control loops. We show some results of using these tools and describe the recent performance of the RF system during our ongoing commissioning phase.

INTRODUCTION

The Cornell-BNL ERL Test Accelerator (CBETA) [1] project currently being commissioned at Cornell University will be the first high-current multi-turn ERL employing Superconducting Radio Frequency (SRF) Linacs operating in CW. The SRF cavities are housed in two cryomodules, one for the injection system and the other is used to execute energy recovery. The injector cryomodule [2] consists of five 2-cell SRF cavities and is configured to provide a total energy gain of 6 MeV to the electron beam for injection into the CBETA return loop. It has been commissioned in multiple stages starting from 2009 and has reached a peak operating current of 70 mA in 2013 [3]. The main linac on the other hand will be used to execute energy recovery and incorporates six 7-cell SRF cavities [4] with a total design energy gain of 36 MeV. In this paper, we describe our progress in commissioning the Main Linac Cryomodule (MLC) for the energy recovery operation in CBETA along with our automated startup procedures.

In the next section, we describe our high level RF setup with results from initial testing of the Solid State Amplifiers and the circulators which provide RF power to the cavities. Then we describe the operating configuration of our cryogenic system which we have optimized for stable operations. After this, we describe our semi-automated RF commissioning procedure in detail and finally, we report our measurements during beam operations over the current commissioning phase.

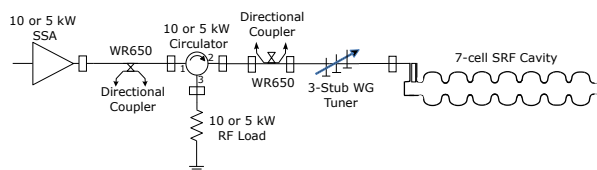


Figure 1: RF power arrangement for one main linac cavity. We inserted a waveguide short between the fundamental power coupler of the 7-cell SRF cavity and the 3-stub waveguide tuner during tests of the solid state amplifiers.

LINAC SUBSYSTEMS

The Main Linac Cryomodule (MLC) houses six 7-cell SRF cavities optimized for high-current operations with negligible beam loading. All six cavities are operated with a low bandwidth of ≈ 20 Hz and are powered by individual Solid State Amplifiers (SSA) from *SigmaPhi* connected through a circulator from *AFT*, directional coupler and a 3-stub waveguide tuner as shown in Fig. 1. There are two sets of high power RF components which are capable of 5 kW and 10 kW for stiffened [5] and un-stiffened cavities respectively. We first tested all these components to full power into a shorted waveguide before connecting them to the cavities. The initial tests revealed problems with both the RF amplifiers and the circulators.

Each SSA requires a power circulator for protection from a full reflection which is close to the typical operating condition. During initial tests we measured both the forward power from the amplifier and the power reflected back into the SSA from the circulator to verify isolation in the RF path. While operating at a few kW of RF power, we observed a sudden jump in the reflected power from ≈ 10 W to ≥ 200 W on all SSAs, which indicated a problem with the circulators. Eventually, we found that a plastic piece used to isolate an aluminum tuning screw from the water-cooled ferrite load had disintegrated during the initial tests, resulting in electrical breakdown and severe pitting in several areas of the load, along with loss of isolation characteristics of the circulator. After consulting with *AFT*, we discovered that the plastic piece installed on the end of the tuning screws had a much higher loss tangent than intended. These were eventually replaced and the load surfaces were cleaned after removing some broken pieces of ferrite. We then tested each circulator at low power with a network analyzer optimizing the isolation. A damaged internal RF cable also led to the failure of a single RF power module on a 5 kW SSA. Figure 2 shows the final measurements after necessary repairs indicating satisfactory performance of all high power RF components.

* This work was supported by the New York State Energy Research and Development Authority, Contract No. DE-SC0012704 with the U.S. Department of Energy and NSF award DMR-0807731.

[†] nb522@cornell.edu

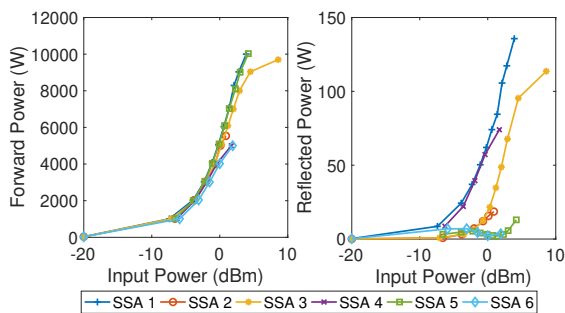


Figure 2: Transfer function measurement of the 6 solid state amplifiers. While odd numbered amplifiers powering unstiffened cavities are capable of reaching a forward power of 10 kW, the even numbered ones power the stiffened cavities with a maximum forward power of 5 kW. The left panel shows the forward power as a function of input power, while the right panel shows the power reflected into the SSA from the circulators.

The cryogenic system of the MLC is based on the TESLA design. [6] Separate vessels house the six cavities and are supplied liquid Helium through chimneys by the 2 K - 2 phase pipe. The pressure exerted on the cavity walls influences the resonant frequency and needs to be regulated. Slow trends in this pressure give rise to very low frequency microphonics detuning ($\lesssim 1$ Hz) and tight cryogenic regulation is necessary during operations. When the RF system is off, two separate proportional integral loops control the Helium liquid level by varying the JT and the precool valves, while we maintain the vapour pressure by adjusting the speed of the external blowers. However actuation of these valves significantly contribute to peak microphonics detuning in the SRF cavities and this is suppressed by making these valves static. When the RF system is operating at low gradients, we set the pump skids to their minimum speed and adjust a bypass needle valve to apply some load to regulate the liquid level. In nominal conditions, the position of the JT valve is set to match the Helium boil off keeping the liquid level constant. One important indicator of cryogenic performance is the speed of the blowers shown in Fig. 3 which has been within acceptable limits with the two blowers connected to the HGRP never exceeding 50% of maximum speed for nominal energy gain of 36 MeV and both reaching 67.5% at the maximum gain of 53 MeV.

RF COMMISSIONING AND PERFORMANCE

Initial commissioning of the MLC after setting up the cryogenic and the high power RF systems, primarily involves tuning the cavities to resonance and setting up the Low Level Radio Frequency (LLRF) control system for optimum operations. In this section we document the procedures we follow to prepare the MLC for beam operations. While we have done the initial commissioning manually, most of these steps are automatically executed for routine operations

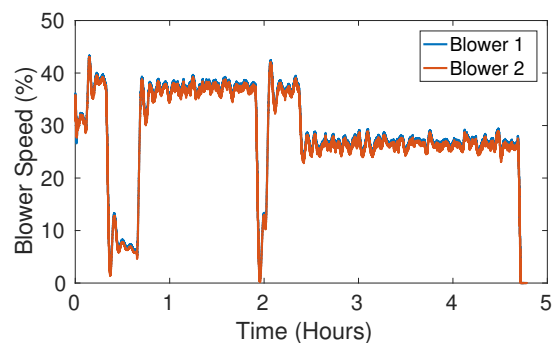


Figure 3: Blower speeds (percentage of maximum) as functions of time during typical 36 MeV RF operations for the FAT.

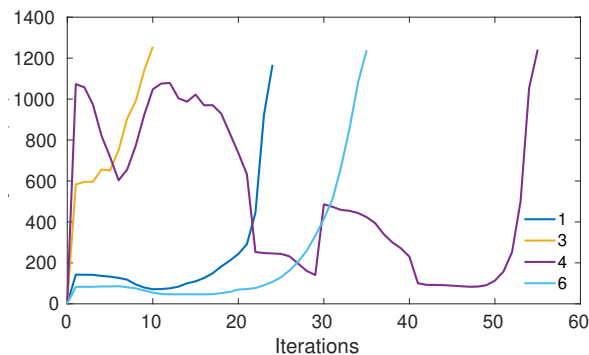


Figure 4: Performance of the automatic coarse tuning algorithm. The graph shows how the accelerating voltage changes as the algorithm progressively tunes four cavities of the main linac to resonance in multiple iterations.

using a dedicated sequencer capable of rudimentary error handling. Such automation has also been used elsewhere [8]. Repeating these procedures everyday accounts for drifts in the system and ensures stable operations.

Step 1: Cavity tuning is the first step towards setting up after cable calibration and we use stepper motor based slow tuners to obtain resonance at the clock frequency of 1299.9 MHz. We first use a network analyzer to tune the cavities within 10 kHz of the clock frequency at low field while we use the LLRF system in constant power mode (called Klystron Loop in the Cornell LLRF [7]) to fine tune the cavity to within a few Hz of resonance on average. During the tuning process, we maximize the field signal while using a forward power of 10 W which gives us the resonance position at an accelerating voltage just above 1.1 MV. The performance of the automatic coarse tuning algorithm based on decision tree approach is shown in Fig. 4. This step allows us to establish the field control loop at a low voltage of around 1 MV, which is a prerequisite for subsequent procedures.

Step 2: The Digital to Analog Converter (DAC) output used in the LLRF system to drive the vector modulator may have some offset due to manufacturing differences. This leads to some non-zero forward power being injected into

Content from this work may be used under the terms of the CC BY 3.0 licence (© 2019). Any distribution of this work must maintain attribution to the author(s), title of the work, publisher, and DOI

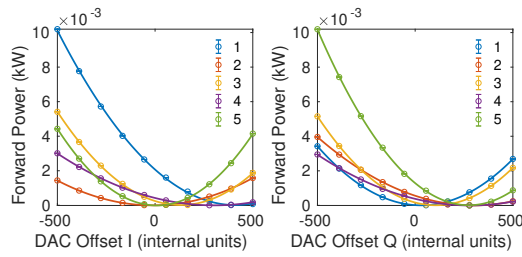


Figure 5: Parasitic forward power as functions of Digital to Analog Converter (DAC) offsets for in-phase I (left panel) and quadrature Q (right panel) components of the output phasor. The plots show data for five main linac cavities and the corresponding quadratic fits, with the minima being the computed offsets.

the cavity even when the output is set to 0 leading to a parasitic field appearing in the cavity when the feedback loop is not active. To account for the offsets, both the in-phase I and the quadrature Q components of the output phasor are shifted by a programmable offset in the LLRF. We measure parasitic forward power as a function of offset as shown in Fig. 5 setting the optimum value at the position of minimum power.

Step 3: The LLRF system implements various trips which turn off RF power going into the cavity in case of a situation which might damage the RF system. Setting the various trip parameters is an important step in commissioning the cavities. There are three categories of trip parameters which we have to set. The SSA trip parameters set the threshold for the maximum power reflected from the circulator into the SSA. The power scale contains a calibration factor while *Max. power* sets the scaled power threshold. The *Power* trip parameters are thresholds on the maximum forward and reflected power, while quench detection relies on a sudden but sustained fractional decrease in reflected power. Finally, we set the *Field* trip parameters which control the maximum field tolerated by the system during normal operations. The important trip parameters and their usage are listed in Table 1.

Step 4: The phase rotation of the field signal due to the cable length between the field probe and the control system influences the stability of the constant field control loop (called Cavity Loop in the Cornell LLRF) and also directly affects measurement of the tuning angle $\phi_t \equiv \phi_{\text{Field}} - \phi_{P_r}$ which is the phase difference between the field signal ϕ_{Field} and the forward power signal ϕ_{P_r} . The detuning δf of the cavity is given by,

$$\delta f = \frac{f_{\text{drive}}}{2Q_L} \tan \phi_t, \quad (1)$$

where Q_L is the loaded quality factor of the cavity, f_{drive} is the clock frequency of the RF system. From Eq. 1 we can conclude that $\delta f = 0 \implies \phi_t = 0$, and this is used to adjust the field rotation offset. We first set the field rotation after manual tuning done in step 1 so that measured tuning angle approximately equals zero when the cavity is in tune. This

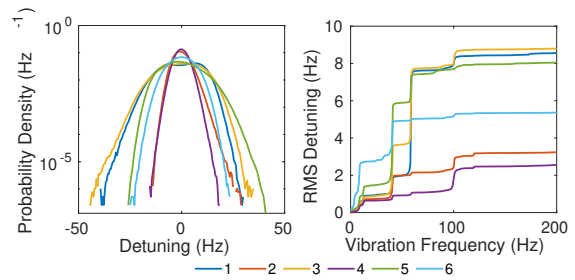


Figure 6: Microphonics measurements on all MLC cavities using the LLRF diagnostic tool. The left panel shows the histogram of detuning while the right panel shows the integrated spectrum.

gives us the rotation value correct to 1-2 degrees. We then observe the average forward power required to maintain a stable field in the cavity (Cavity Loop) as a function of the tuning angle ϕ_t set point of the resonance control feedback loop. The position of minimum forward power corresponds to a perfectly tuned cavity, and the phase rotation is adjusted accordingly.

Step 5: Microphonics poses a major constraint on field stability for the MLC cavities which we operate with high Q_L as noted in the previous section. The LLRF system provides a tool to measure the microphonics in the system as shown in Fig. 6. The LLRF measures the peak forward power and detuning with a time resolution of $10 \mu\text{sec}$ and $100 \mu\text{sec}$ respectively. We ensure that the peak microphonics detuning is $\leq 50\text{Hz}$ for stable operations while the peak power should be less than the maximum output of the SSA connected to the cavities, 5 kW for stiffened and 10 kW for un-stiffened. If deemed necessary, we can use the spectrum measurement to determine the frequencies of strong vibrations in the cryomodule and then activate the ANC algorithm on these sources.

Step 6: Stability of electric field in the RF cavity depends on the proportional and integral gains of the field control loop (cavity Loop). We complete steps 4 and 5 with some default parameters for the control loop, namely with a normalized proportional gain of about 100 and a zero integral gain. Then we measure the standard deviation of the field amplitude and phase as a function of the feedback gains in order to optimize the performance of feedback control.

CONCLUSION

The MLC housing six 7-cell cavities will be used for energy recovery in CBETA with a nominal accelerating voltage of 6 MV on each cavity. Three of these cavities are fitted with stiffening rings in order to reduce their sensitivity to external vibrations. The vibrations in this TESLA style cryomodule drive large microphonics detuning of the SRF cavities comparable to their bandwidth thus limiting the field stability in the presence of available maximum RF power. Keeping this in mind, the un-stiffened cavities are powered by SSAs capable of generating 10 kW while the others can generate 5 kW. Initial testing of the high power

Table 1: Trip parameters used in each SRF cavity of the main Linac.

Category	Name	Units	Description
SSA	SSA Refl Power Scale	kW/count ²	Calibration factor for power reflected from the circulator into the SSA.
Power	Max. power	kW	Maximum power threshold for SSA trip.
	Cavity Fwd Power Scale	kW/count ²	Calibration factor for forward power into the cavity.
	Scale Factor Ratio Refl to Fwd		Ratio of reflected and forward power calibration factors.
	Max. Forward Power	kW	Maximum forward power threshold for Cavity Max Forward trip.
	Max. Reflected Power	kW	Maximum reflected power threshold for Cavity Max Reflected trip.
	Fractional Decrease Trip Level		The fractional decrease threshold for reflected power for a Cavity Reflected Quench trip.
	Max. Loop Count	Units of 10 μ s	Time to wait before declaring a Cavity Reflected Quench trip.
Field	Field Square Scale	(kV/count) ²	Calibration factor for square of field.
	Field Amp Sq	(kV) ²	Threshold for Max Cavity Power trip.

RF components led to failure of the circulators, eventually traced to a manufacturing defect originating from a material with a high loss tangent. One of the RF amplifier slices also failed during initial testing due to large reflected power from a faulty connector damaging the sensitive transistors. After repair all RF components are operating normally and we have tested everything to full power. We also carefully optimized various cryogenic system control loops which regulate Helium level and pressure inside the cryomodule in response to varying levels of thermal load during RF operations. The performance of the room temperature Helium blowers which maintain 2 K vapour pressure inside the cryomodule strongly suggests that the thermal dissipation of the cavities is within the expected range.

The RF system commissioning involves tuning all cavities to resonance and setting various LLRF control parameters to ensure stable operations. Once the system was sufficiently optimized in the initial days of operations, we have automated many of these steps which are run by a sequencer everyday before starting beam operations. We start by tuning the cavities to resonance using the slow tuner system, followed by reducing the leakage of forward power into the cavities by optimizing the offsets of the LLRF DACs. Then we set the parameters which allow the LLRF to safely trip off, protecting the system from permanent damage. After this, we close the feedback loop to maintain a stable field of 1 MV inside the cavity, and measure the phase offset of the field probe signal. Finally we measure microphonics and field stability and optimize the field and resonance control loops for stable operations. Future work will involve automating steps 5 and 6 of the startup procedure with special emphasis on establishing stable high-current energy recovery operations with no spontaneous trips.

ACKNOWLEDGEMENTS

We would like to thank Dan Sabol and Colby Shore for setting up the cryogenic systems for both cryomodules and help in optimizing the Helium control loops. We would also like to acknowledge Adam Bartnik and Colwyn Gulliford

for devoting a substantial amount of time towards operations. This work was supported by the New York State Energy Research and Development Authority. This manuscript has been authored by employees of Brookhaven Science Associates, LLC under Contract No. DE-SC0012704 with the U.S. Department of Energy. CLASSE facilities are operated with major support from the National Science Foundation.

REFERENCES

- [1] G. H. Hoffstaetter *et al.*, "CBETA, the 4-Turn ERL with SRF and Single Return Loop", in *Proc. IPAC'18*, Vancouver, Canada, Apr.-May 2018, pp. 635–639. doi:10.18429/JACoW-IPAC2018-TUYGBE2
- [2] M. Liepe, G. H. Hoffstaetter, S. Posen, P. Quigley, and V. Veshcherevich, "High Current Operation of the Cornell ERL Superconducting RF Injector Cryomodule", in *Proc. IPAC'12*, New Orleans, LA, USA, May 2012, paper WEPPC072, pp. 2378–2380.
- [3] B. Dunham *et al.*, "Record high-average current from a high-brightness photoinjector", *Appl. Phys. Lett.*, vol. 102, p. 034105, Jan. 2013.
- [4] F. Furuta *et al.*, "Performance of the Novel Cornell ERL Main Linac Prototype Cryomodule", in *Proc. LINAC'16*, East Lansing, MI, USA, Sep. 2016, pp. 492–495. doi:10.18429/JACoW-LINAC2016-TUPLR011
- [5] S. Posen and M. Liepe, "Mechanical optimization of superconducting cavities in continuous wave operation", *Phys. Rev. ST Accel. Beams*, vol. 15, p. 022002, Feb. 2012.
- [6] E. N. Smith, Y. He, G. H. Hoffstaetter, M. Liepe, and M. Tigner, "Cryogenic Distribution System for the Proposed Cornell ERL Main Linac", in *Proc. IPAC'12*, New Orleans, LA, USA, May 2012, paper MOPPP026, pp. 619–621.
- [7] A. Neumann *et al.*, "CW Measurements of Cornell LLRF System at HoBiCaT", in *Proc. SRF'11*, Chicago, IL, USA, Jul. 2011, paper MOPO067, pp. 262–266.
- [8] Z. Q. Geng, "RF Control Optimization and Automation for Normal Conducting Linear Accelerators", in *IEEE Transactions on Nuclear Science* vol. 64, no. 8, pp. 2361–2368, Aug. 2017.